

Research Paper

The Mass and Speed Dependence of Meteor Air Plasma Temperatures

PETER JENNISKENS,¹ CHRISTOPHE O. LAUX,^{2,*} MICHAEL A. WILSON,³
and EMILY L. SCHALLER^{4,†}

ABSTRACT

The speed and mass dependence of meteor air plasma temperatures is perhaps the most important data needed to understand how small meteoroids chemically change the ambient atmosphere in their path and enrich the ablated meteoric organic matter with oxygen. Such chemistry can play an important role in creating prebiotic compounds. The excitation conditions in various air plasma emissions were measured from high-resolution optical spectra of Leonid storm meteors during NASA's Leonid Multi-Instrument Aircraft Campaign. This was the first time a sufficient number and range of temperature measurements were obtained to search for meteoroid mass and speed dependencies. We found slight increases in temperature with decreasing altitude, but otherwise nearly constant values for meteoroids with speeds between 35 and 72 km/s and masses between 10^{-5} g and 1 g. We conclude that faster and more massive meteoroids produce a larger emission volume, but not a higher air plasma temperature. We speculate that the meteoric plasma may be in multiphase equilibrium with the ambient atmosphere, which could mean lower plasma temperatures in a CO₂-rich early Earth atmosphere. **Key Words:** Prebiotic molecules—Origin of life—Meteors—Plasma temperatures—Multiphase medium. *Astrobiology* 4, 81–94.

INTRODUCTION

INFALLING EXOGENOUS MATTER responsible for meteors is capable of altering the atmospheric composition in its wake, creating compounds such as NO that are important for nitrogen fixation. In the process, the mixture of air plasma and

ablation products can chemically change the organic molecules ablated from the meteoroid (Jenniskens *et al.*, 2004). Meteoroids ~150 μ m in size represented a significant source of mass influx at the time of the origin of life, rivaling the amount of material delivered by less frequent comet and asteroid impacts (Chyba and Sagan, 1992; Love

¹Center for the Study of Life in the Universe, SETI Institute, Mountain View, California.

²High Temperature Gasdynamics Laboratory, Mechanical Engineering Department, Stanford University, Stanford, California.

³NASA Ames Research Center, Moffett Field, California.

⁴NASA Ames Astrobiology Academy, Dartmouth College, Hanover, New Hampshire.

*Present address: Ecole Centrale Paris, Laboratoire EM2C, Chatenay-Malabry, France.

†Present address: Astronomy Department, California Institute of Technology, Pasadena, California.

and Brownlee, 1993; Jenniskens *et al.*, 2000). Today, only a small mass fraction (<8%) of meteoroids in the 10–50 μm range survive entry in Earth's atmosphere and arrive unaltered as micrometeorites (Anders, 1989). An even smaller fraction of large meter-size asteroidal debris survives in the form of meteorites. The bulk of infalling meteoroids is ablated in the Earth's atmosphere, and in the process creates brief flashes of light called meteors.

Some of the relevant chemistry occurs in a warm ($T \sim 4,400$ K) air plasma, thought to result from expansion into the ambient atmosphere of impinging air molecules after their interaction with the meteoroid and its ablation vapor cloud (Boyd, 2000; Jenniskens *et al.*, 2000; Popova *et al.*, 2000). The physical conditions in this plasma set the tone for the subsequent chemical evolution of ablated compounds and the atmosphere in the meteor's path. The initial impact excitation is a highly non-local thermodynamic equilibrium (LTE) process, but the product is a warm plasma with air plasma and metal atom emissions that are nearly in equilibrium (Jenniskens *et al.*, 2000). From this plasma, the site of the bulk of hot-temperature chemistry, the bulk of optical emissions is observed. The plasma only gradually cools with distance away from the meteoroid (Jenniskens and Stenbaek-Nielsen, 2004).

Earlier excitation temperature measurements, summarized in Table 1, were based on analysis of the curve of growth of radiation from metal ablation lines in photographic spectra of bright fireballs (Ceplecha, 1964, 1968; Harvey, 1973). The brighter metal atom lines of meteors as faint as +0 magnitude are affected by self-absorption and damping, due to significant absorption of emitted photons in the plasma itself (Ceplecha, 1973). Values of the metal atom excitation temperature of such fireballs were calculated to range from 3,000 to 5,500 K, with no obvious dependency on meteor velocity or mass. The only significant dependence was noticed by Ceplecha (1965), who found a decrease in the excitation temperature as a function of meteor luminosity during a flare. However, these and other measurements of temperature are model dependent, with early measurements later corrected upwards, to match the luminous efficiency, by assuming that the effective radiating volume increases with decreasing lower energy level of the excitation. The adjusted values were around 5,500 K and pertain to bright fireballs at a typical altitude of 75 km and speed 32 km/s (Ceplecha, 1973).

More recent excitation temperatures were derived by fitting synthetic spectra of optically thin radiation (*i.e.*, no self-absorption) to the metal atom ablation lines (Borovička, 1993). Borovička (1994) concluded that several lines, including Ca^+ and Mg^+ , originate from a separate hot gas component with $T \sim 10,000$ K. This high-temperature plasma makes up only 0.02% (in number, not volume) of the meteor vapor envelope in slow meteors but accounts for more than 5% in fast meteors. Borovička (1994) considered the O and N atomic lines in meteor spectra to be part of this high-temperature gas because of their high excitation energies (11–12 eV). Moreover, results from curve of growth analysis of atomic oxygen lines by Ceplecha (1973) also pointed to an air plasma temperature of about 14,000 K.

The recent introduction of cooled charge coupled device (CCD) detectors in meteor spectroscopy (Jenniskens *et al.*, 2000) provides the near-infrared sensitivity and detector linearity necessary to derive air plasma temperatures from the shape of the first positive bands of molecular N_2 (first identified by Cook and Millman, 1954) and the relative intensity of the O and N atomic lines. From the first such spectra recorded during the 1998 Leonid Multi-Instrument Aircraft Campaign (MAC) (Jenniskens and Butow, 1999), we found that the chemical equilibrium of N and N_2 was well described by an LTE temperature of about $T \sim 4,300$ K. This happens to coincide with the chemically most interesting temperature domain in air plasma chemistry for a CO_2 -rich early Earth atmosphere, making meteors a relatively efficient source of reduced molecules in an oxidizing atmosphere (Jenniskens *et al.*, 2000).

Here, we use the same measures of temperature to consider the mass and speed dependence at the peak of optical luminosity. Extrapolation to smaller sizes provides the relevant conditions for meteoroids that supply most of the mass influx, which are particles ~ 150 μm in size with a median speed of about 25 km/s, rather than the much brighter or faster meteors that can be measured by optical techniques.

METHODS

A large sample of high-quality Leonid spectra were measured during the 2001 Leonid MAC (Jenniskens and Russell, 2003), all of which entered the Earth's atmosphere at 71.6 ± 0.4 km/s.

TABLE 1. SUMMARY OF CURVE-OF-GROWTH TEMPERATURE MEASUREMENTS FROM METAL ATOM LINE EMISSIONS FOUND IN THE LITERATURE

Meteor	M _v	magnitude	V _{inf} (km/s)	H (km)	T (K)		Method ^a	Reference
					Warm	Hot		
Cometary S6		-12	22	76	2,970 ± 160	7,600	c-Fe I Ca/Ca ⁺ Saha	Ceplecha (1964) Ceplecha (1964)
EN39421		-3	32.6	75	3,990 ± 80 4,380 ± 100 5,280 ± 60 4,120 ± 200		Fe I no wake c-Ca I c-Na I c-O I c-Fe I	Ceplecha (1971) Ceplecha (1971) Ceplecha (1971) Ceplecha (1971) Ceplecha (1971)
Sample EN 151068		-	-	-	5,490 ± 130 3,500-6,000 3,500-4,700	14,000 ± 3,000	? s-Fe, Ca, Mg s-O I, N I	Harvey (1971) Borovička (1993) Borovička (1993)
α-Capricornid Sumava (1974)		-05 -22	23 -	84 59	3,600 4,000-5,000	10,000	s-Fe, Mg s-Fe, Ca, Mg	Borovička and Weber (1996) Borovička and Spurný (1996)
Perseid		-11	61	~85	4,400-4,800 ^b		s-Fe, Mg, Na s-Ca II, O I	Borovička and Betlem (1997) Borovička and Betlem (1997)
Perseid		-05	61	~85	4,500 ^b	10,000 ^b	s-Fe I, Mg I s-O I, N ₂	Borovička and Majden (1998) Borovička and Majden (1998)
Asteroidal EN32281		-10	28.9	71	2,900-3,650		c-Fe I	Ceplecha (1965)
EN36221 (iron)		-10	31.9	75	3,195/5,350 5,500 ± 370		c-Fe I c-Fe I	Ceplecha (1967) Ceplecha (1973)
EN 130960		-11	30	75	5,540 ± 160		c-Fe I	Ceplecha (1973)
EN 32281		-10	28.9	75	5,510 ± 200		c-Fe I	Ceplecha (1973)
EN 070591		-20	21	24	4,000-6,000		s-Fe I, Ca I	Borovička <i>et al.</i> (1998)

^ac, curve of growth; s, synthetic spectrum fit to data.

^bAssumed.

TABLE 2. NEW TEMPERATURE (IN K) MEASUREMENTS DERIVED FROM THE O, N, AND N₂ AIR PLASMA EMISSIONS SHOWN IN FIG. 2

Source	Time (UT)	pO I (FW)	V _{inf}	T _{vib} N ₂	T _c N I (747/742)	T _{chem} N I/N ₂			T _{chem} O I/N ₂			
						N 747	N 822	N 868	O 777	O 845	O 616	
Geminid 2001	07:15:28	4,700 (0.7)	36	4,700 ± 100	—	4,310 ± 10	—	—	—	—	—	~4,700
Perseid 1999	10:35:26	5,425 (1.3)	61	4,670 ± 200	—	4,345 ± 10	—	—	—	—	—	~4,710
Perseid 1999	07:52:38	5,300 (1.2)	61	4,700 ± 200	4,100 ± 300	4,320 ± 10	—	—	4,395	—	—	~4,710
Perseid 2000	07:00:57	2,260 (0.7)	61	—	—	4,320 ± 20	—	—	4,340	—	—	—
Leonid 1998	17:40:54	96 (0.6)	72	—	—	—	4,435 ± 20	4,455 ± 30	—	—	4,380	—
Leonid 1998	17:47:06	235 (0.75)	72	—	—	4,340 ± 20	—	4,400 ± 20	—	—	4,310	—
Leonid 1998	18:08:46	10,300 (0.4)	72	—	—	—	—	4,420 ± 30	—	—	4,240	—
Leonid 1998	19:56:13	50 (0.7)	72	—	—	4,400 ± 50	4,440 ± 20	—	—	—	4,270	—
Leonid 2001 ^a	09:05:57	170 (0.6)	72	—	—	—	—	—	—	—	—	4,540
Leonid 2001 ^a	09:19:05	5,400 (0.4)	72	6,050 ± 200 ^b	—	4,376 ± 10	—	—	—	—	—	4,650
Leonid 2001 ^a	09:42:25	3,130 (0.8)	72	6,120 ± 100	4,355 ± 20	—	—	—	—	—	—	—
Leonid 2001	10:04:30	568 (0.7)	72	—	—	—	4,480 ± 10	4,460 ± 30	4,400	—	—	—
Leonid 2001	10:15:16	325 (0.8)	72	—	—	4,380 ± 10	4,336 ± 10	4,340 ± 10	4,303	—	—	—
Leonid 2001	10:44:58	600 (0.9)	72	4,450 ± 50	4,430 ± 50	—	4,475 ± 10	—	4,310	—	—	—
Leonid 2001	10:47:02	3,860 (0.4)	72	—	—	—	—	4,500 ± 40	—	—	—	—
Leonid 2001	10:52:31	620 (0.9)	72	5,590 ± 50 ^b	—	—	—	—	—	—	—	4,470
Leonid 2001	10:56:43	203 (0.6)	72	—	—	—	4,580 ± 20	4,590 ± 20	4,420	—	—	—
Leonid 2001	11:11:00	148 (0.75)	72	—	—	—	4,455	4,486	4,400	—	—	—
Leonid 2001	11:32:43	48 (0.6)	72	—	—	4,430 ± 50	4,530	—	4,440	—	—	—
Leonid 2001	11:33:49	164 (0.4)	72	—	—	—	4,500	4,570	4,380	—	—	—
Leonid 2001 ^a	12:35:06	1,686 (0.55)	72	—	4,320 ± 10	4,347 ± 10	—	—	4,416	—	—	—

FW, full width at half maximum.

^aSecond order.^bContamination from CaO.

In addition, a small number of spectra from the annual Perseid (60.6 ± 0.6 km/s) and Geminid (36.3 ± 0.6 km/s) showers were measured in recent ground-based campaigns, which are included in order to address the issue of the dependence of excitation temperatures on meteoroid speed. The two-stage thermoelectrically cooled CCD slit-less meteor spectrograph for astronomy and astrobiology (“ASTRO”) and its instrumental properties are described in detail in Jenniskens *et al.* (2004). In summary, a Pixelvision camera with two-stage thermoelectrically cooled $1,024 \times 1,024$ pixel back-illuminated SI003AB CCD with 24×24 μm pixel size (24.5×24.5 mm image region) was used in un-intensified mode to keep as high a spectral resolution as possible. To limit the readout time (dead time) to less than 1 s, we recorded images with $4\times$ binning in the direction perpendicular to the dispersion direction. The imaging optics was an AF-S Nikkor f2.8/300D IF-ED 300-mm telephoto lens, which provided a field of view of $5 \times 5^\circ$. In front of the lens was mounted an 11×11 cm plane transmission grating (#35-54-20-660 by Richardson Grating Laboratory, Rochester, NY, with aluminum coating) on a 12-mm BK7-type glass substrate. We measured a dispersion of $540 \text{ \AA}/\text{mm}$ and a blaze wavelength of 698 nm (34°). This configuration provided a full second order spectrum out to about 925 nm.

RESULTS

ASTRO was deployed onboard the U.S. Air Force 418th Flight Test Squadron-operated NKC-135 “FISTA” research aircraft over the continental United States during the 2001 Leonid MAC

mission at the time of the intense November 18 10:40 universal time (UT) Leonid storm peak (Jenniskens and Russell, 2003). This storm was caused by dust released from the 1767 return of comet 55P/Tempel-Tuttle. Twenty-three high-resolution spectra were obtained, 13 of which contain one of the First Positive bands of N_2 . This sample dataset (Table 2, which includes four spectra from the 1998 Leonid MAC mission and four spectra from ground-based campaigns during the Perseids and Geminids) more than doubled the number of available spectra from prior missions and ground-based campaigns. While Table 1 provides data for -5 to -22 magnitude fireballs, the newly acquired data are for fainter meteors of magnitude $+3$ to -2 . Each spectrum covers a spectral range of about 200 nm, with a central wavelength determined by the position of the meteor on the sky relative to the viewing direction of the camera.

Figure 1 shows the raw data of one of our best results, a Leonid meteor spectrum in second order that is centered on the $\Delta\nu = +2$ First Positive band of N_2 , meaning the transitions from the $B \rightarrow A$ electronic state of N_2 that also correspond to a change of $+2$ in the vibrational quantum number (Herzberg, 1950). The meteor moved from bottom to top. The images from background stars were removed by subtracting an image taken shortly after the meteor. On top of the broad diffuse emission of N_2 are lines of atomic nitrogen. Nearly all of the detail in this spectrum is due to the various rovibrational transitions in the nitrogen molecule. Atomic lines from ablated metal atoms are few and faint in this part of the spectrum.

Figure 2 shows the reduced spectra, derived from data such as that shown in Fig. 1, acquired

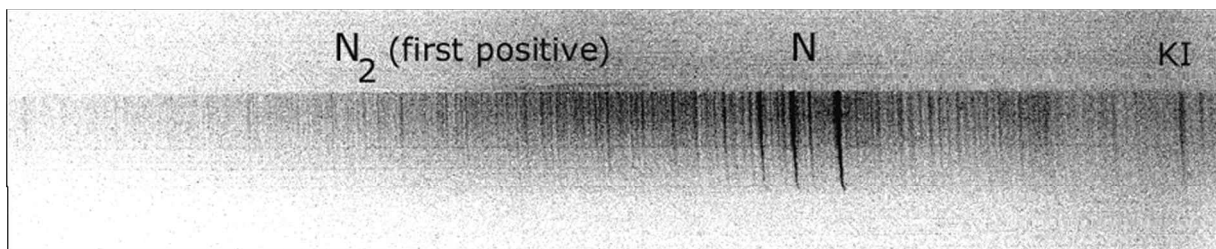


FIG. 1. Spectrum of the 09:42:25 UT Leonid meteor in the range 699–768 nm in second order. Most emission lines are rotational and vibrational structure in the $\Delta\nu = +2$ First Positive band of molecular nitrogen. Superposed are emission lines from atomic nitrogen and some meteoric metal atoms, including third order lines of iron (466–512 nm). Background star images have been removed. The wavelength scale runs left to right; the meteor moved from bottom to top, increasing in brightness. The spectrum is terminated by the end of the exposure.

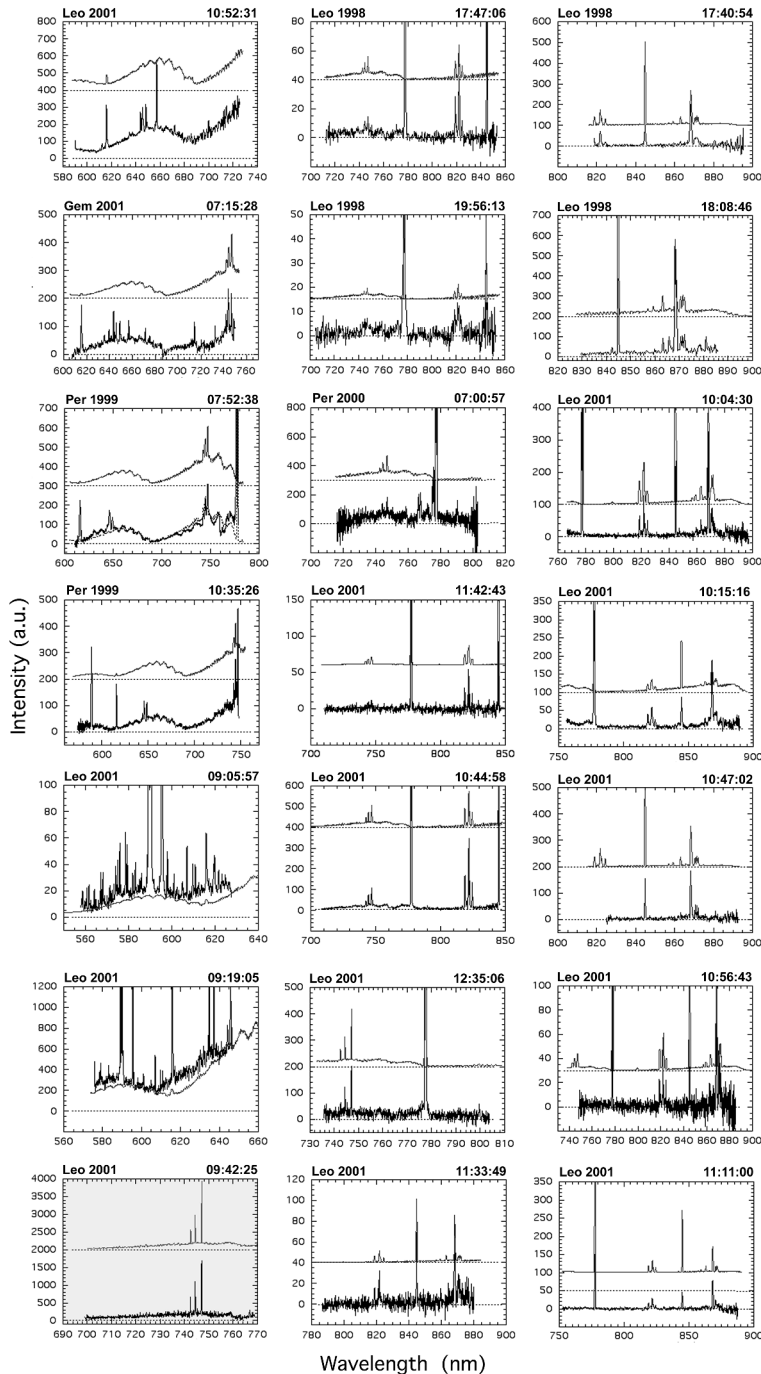


FIG. 2. Meteor spectra containing one of the N_2 First Positive bands. Each graph shows the meteor intensity corrected for instrument response versus wavelength (nm) in arbitrary units. Superposed is a model spectrum, displaced upward for clarity.

during the 1998 (4) and 2001 (13) missions, and during the 1999 (2) and 2000 (1) Perseid and 2001 (1) Geminid ground campaigns. Superposed on each reduced spectral plot shown in Fig. 2 is the calculated emission line spectrum for N_2 , as discussed in the next section. The data reduction process is described in Jenniskens *et al.* (2004). In summary, each spectrum was reduced by (1) sub-

tracting a background frame taken a second after the meteor to remove stars and dark current, (2) correcting the rows for vignetting (flatfielding), (3) removing cosmic ray hits and star residues, (4) aligning and averaging the CCD rows to correct for the meteor's motion relative to the direction of dispersion, and (5) correcting the resulting one-dimensional spectrum for the instrument

spectral response function. The spectrum obtained by reducing the image of Fig. 1 is shown in the lower left corner of Fig. 2.

The $B \rightarrow A$ electronic state of N_2 is shown in the energy diagram of Fig. 3. The different ranges of wavelengths in individual spectra cover the different changes in vibrational quantum numbers between upper and lower state $\Delta v = +1$ (860 nm), $+2$ (770 nm), $+3$ (680 nm), and $+4$ (590 nm) bands from the First Positive band system of N_2 (Herzberg, 1950). Superposed on the N_2 bands are groups of atomic nitrogen lines at ~ 746 nm, 822 nm, and 869 nm, and unresolved groups of atomic oxygen at 615.8 nm, 777.3 nm, and 844.7 nm. Only the Leonid spectra, which were obtained at altitude, are free of water bands originating from absorption in the Earth's atmosphere (called telluric), which cover significant parts of the near-infrared spectrum. In addition, all spectra near 760 nm contain the telluric oxygen A band, while ground-based observations also show the telluric oxygen B band at 680 nm.

Temperature measurements

Each reduced spectrum was then compared with the spectrum generated using an air plasma emission model. The expected relative abundance for each relevant compound was calculated by as-

suming LTE for an air plasma in equilibrium with its surroundings at a pressure of 10^{-6} atmospheres (95 km altitude). The expected emission intensities of the First Positive bands of N_2 and the atomic nitrogen and oxygen lines were calculated with the NEQAIR2 program (as updated in Laux, 1993), and using the 1966 National Bureau of Standards database of Einstein coefficients for the atomic lines. The results were compared with emission intensities calculated with an updated SPECAIR program, which contains the more modern 1996 NIST database (C.O. Laux *et al.*, manuscript in preparation). The latter showed differences of 20–30% in the Einstein coefficients of the relevant N I lines, leading to systematically lower temperatures by 20–40 K.

The next step in the data analysis involved matching the calculated N_2 molecular band to the observed spectrum, and subsequently matching the atomic emission lines relative to the best fit of the N_2 band (*i.e.*, shown as superposed plots for each example shown in Fig. 2). For each emission line, a best-fit temperature was calculated from interpolated intensities in the spectrum at 4,100, 4,300, 4,500, and 4,670 K. The best-fit interpolated temperature T_{int} was calculated by matching the sum of intensities expected for each temperature component to the observed spectrum:

$$T_{\text{int}} = -\frac{E}{k} / \ln \left\{ \frac{a(-E/kT_a) + b(-E/kT_b)}{a + b} \right\} \quad (1)$$

where E is the upper energy level, T_a and T_b are the lower and higher temperature, and a and b are constants used to find the interpolated means. The results are summarized in Table 2. Results differ slightly from those of Jenniskens *et al.* (2000) because of a better treatment of the instrument response functions. Small errors in the position of the N_2 band result in systematic differences in all of the emission line temperatures for a given spectrum. In general, the calculated temperatures were determined to vary within a small range for each diagnostic, in most cases less than ± 100 K, with small systematic variations on the order of 100 K between different diagnostic emission line (and band) ratios. For example, the 845 nm line of O I (relative to the N_2 band strength) suggests a lower temperature than the 822 nm line of N I. These temperatures are thought to describe the chemical equilibrium in

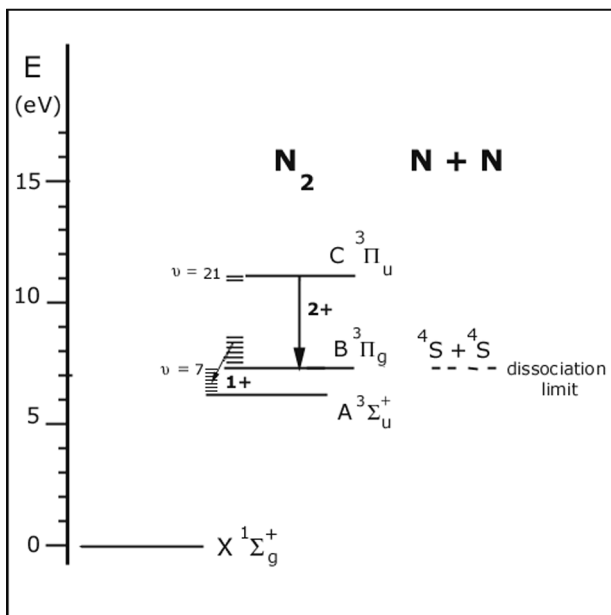


FIG. 3. Simplified energy level diagram of the nitrogen molecule. The First Positive band originates in the $B \rightarrow A$ transition.

the plasma, which determines the abundances of the various compounds.

Another temperature measurement follows from the shape of the band profile itself. Each band is well resolved, with band heads from individual vibrational transitions. The $\Delta\nu = +2$ band in Fig. 2, for example, has peaks representing the vibrational (0,2), (1,3), (2,4), *etc.*, transitions, the width of each peak determined by the molecule's rotational level populations. The slope of the molecular band at high vibrational levels changes slightly with increasing vibrational temperature of the N_2 molecule. The intensity slope at low wavelengths is proportional to the population distribution of the vibrational levels. By fitting the low wavelength slope of the band to the model spectra, we were able to estimate the vibrational temperature of N_2 (Fig. 4).

Some of our spectra showed enhanced emission in the $\Delta\nu = +2$ band contour at short wavelength above that expected from LTE. At least in some of these cases, we suspect that excess emission near 620 nm (Fig. 2) may be molecular emission from CaO, which peaks at 620 nm. FeO emission may be present as well. Indeed, these suspected oxide emission bands are strong in those meteor spectra that have a strong metal atom line component (indicated by footnote b in Table 2). Such contamination can result in misleading results for the vibrational temperature.

Finally, we measured electronic excitation temperatures for the nitrogen lines from the relative

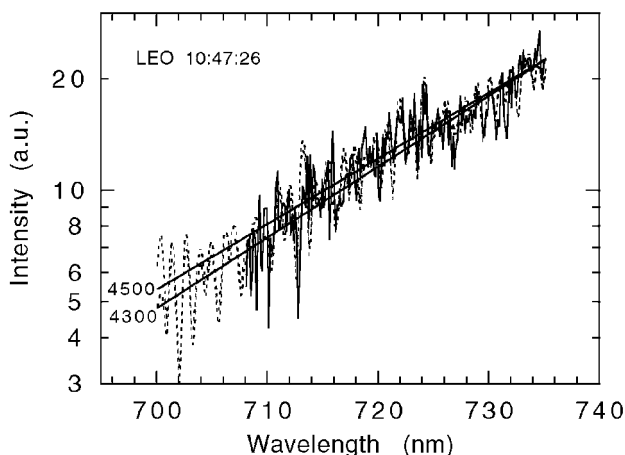


FIG. 4. Variation of the shape of the model N_2 band profile for different assumed vibrational temperatures. Models at 4,500 and 4,300 K are superposed on the observed spectrum of the 10:47:26 UT Leonid meteor of November 18, 2001.

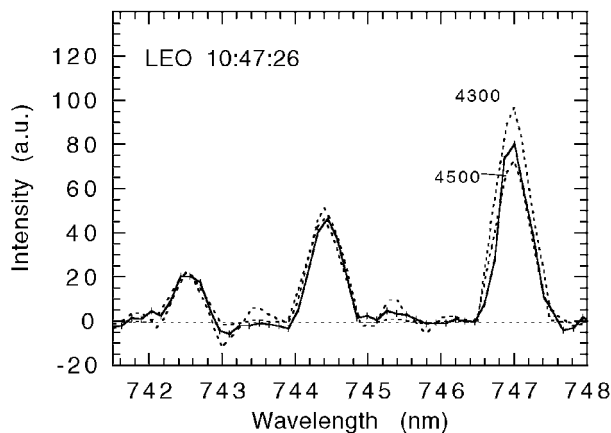


FIG. 5. Response of the N I line ratio to variations in the electronic excitation temperature. The observations of the 10:47:26 UT Leonid meteor of November 18, 2001, after subtraction of the N_2 band profile, are compared with LTE models at 4,300 and 4,500 K.

line intensity ratio of the 746 nm N I lines. The main $3p^4p-3p^4s$ transitions (vacuum wavelengths 742.57, 744.43, and 747.04 nm) have the same 12.00 eV excitation energy, but there are small contributions from higher levels at 13.67 eV. These lines are so close together in the spectrum that small errors in the instrument response and flatfielding have no effect on the outcome. This is important because the observed variations are small (Fig. 5).

In principle, the O I lines at 777 nm (10.74 eV) and 845 nm (10.99 eV) could be used to measure

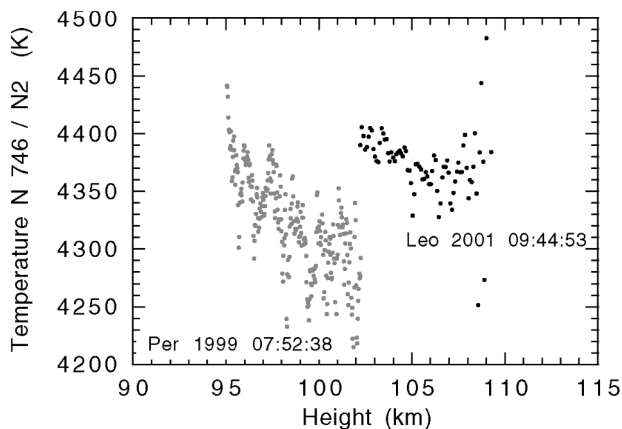


FIG. 6. Gradual increase of temperature with decreasing height as observed from the variation of the N/N_2 intensity ratio (expressed as the corresponding temperature in an LTE model) as a function of height for two meteors.

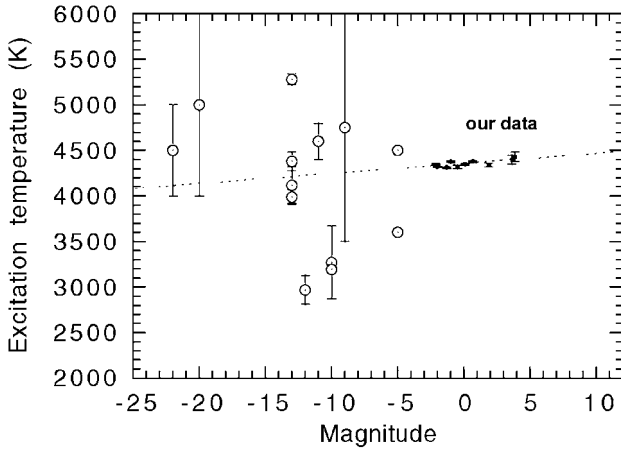


FIG. 7. Temperature as a function of meteor peak visual magnitude. Small dots show our results, while large symbols are data reported in the literature. Literature data are derived from curve-of-growth analysis of metal atom ablation emissions and fits of optically thin emission to meteor spectra (Table 1).

the electronic excitation temperature of oxygen atoms (Park *et al.*, 1997), but those lines are far enough apart in wavelength to be sensitive to any potential intensity calibration uncertainties. Moreover, only four of our spectra show both oxygen lines. The 616 nm line has a significantly higher excitation energy (12.75 eV), but it was not measured simultaneously with the other O I lines.

Temperature dependencies with height, mass, and speed

The various temperatures derived here are mean values for a part of the meteor trajectory,

in particular that part of the trajectory that was bright enough to be recorded. This tends to coincide with the peak of the meteor’s luminosity near 85–115 km.

There was a small gradual increase in the plasma temperature with altitude, judging from the relative increase in the strength of the N I lines. Figure 6 shows results for the 2001 Leonid of 09:42:25 UT (Fig. 1) and the 1999 Perseid spectrum at 07:52:38 UT. The observed trend (between 115 and 85 km) was: T (K) $\sim -7.0 \times H$ (km).

We find that all temperatures derived from the N I/ N₂ ratio were in a small range from 4,300 to 4,700 K, with most results between 4,300 and 4,400 K. All results are summarized in Fig. 7 as a function of visual peak magnitude of meteor brightness. The observed trend with meteor magnitude was very weak. Earlier data summarized in Table 1 are also shown. Those early data scatter widely, but center around the same value.

The brightness (and meteoroid mass) dependence of the chemical equilibrium temperatures for individual nitrogen and oxygen lines, in relation to the molecular band of nitrogen, is summarized in Fig. 8. Each set of data showed a gradual increase of temperatures to smaller meteor brightness, but the trend is very weak, with a slope of only about +15 K/magnitude (Table 3). The result disagreed significantly with the results of Cepelcha (1964), who derived a 10 times steeper dependence versus peak bolometric magnitude from the variation of excitation temperature in the flare of a bright fireball: T (in K) = $(4,427 \pm 399) + (151 \pm 47)M$ (in magnitude).

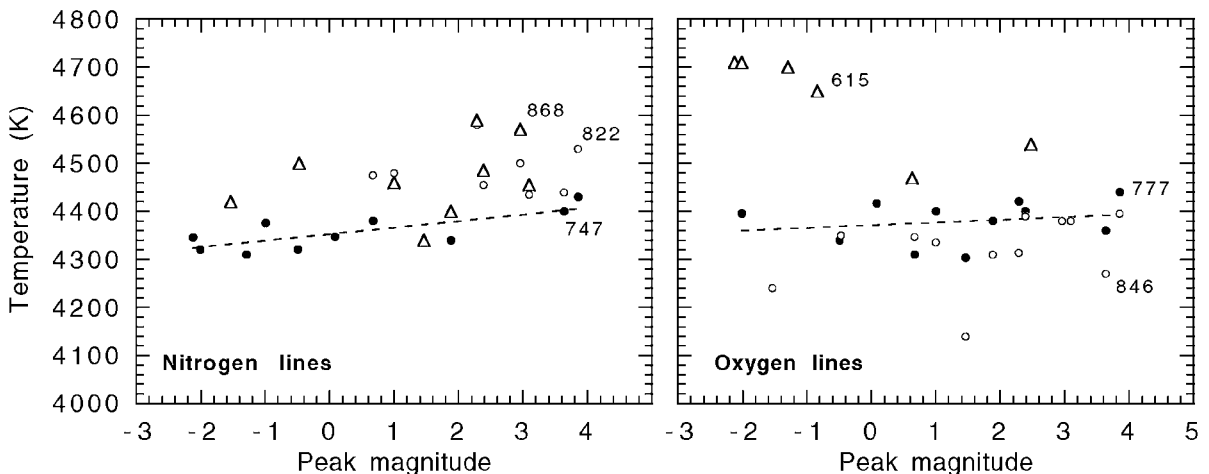


FIG. 8. Chemical equilibrium temperatures as a function of the meteor peak visible magnitude. Right panel: Results from oxygen lines at 616, 777, and 845 nm. Left panel: Results from nitrogen lines at 747, 822, and 868 nm.

TABLE 3. TEMPERATURE (IN K) DEPENDENCE AS A FUNCTION OF MAGNITUDE FOR CHEMICAL EQUILIBRIUM LINE RATIOS RELATIVE TO MOLECULAR NITROGEN EMISSION

	E_j (eV)	Intensity (arbitrary units)	T (m = 0)	$\Delta T/magnitude$	Correlation coefficient
N I 747	12.00	85	4,352	13.7	0.77
N I 822	11.84	320	4,440	13.0	0.22
N I 868	11.76	1,480	4,446	15.6	0.31
O I 616	12.75	50	4,633	-38.0	0.84
O I 777	10.74	1,700	4,371	5.6	0.22
O I 845	10.99	880	4,293	15.7	0.75

The temperatures calculated for the vibrational excitation of N_2 , electronic excitation for N, and the chemical equilibrium temperatures were found to be very similar (Fig. 9). This result implies that the air plasma is nearly in LTE.

Small deviations from LTE were determined to be present in the data. The O I 777 and 865 nm lines were systematically weaker than predicted from an LTE plasma, while the O I 616 nm line is stronger (Fig. 8). Such deviations are important, because they refer to the most common components in the air plasma. Less abundant compounds, including organic molecules from the meteor ablation, exhibited a chemistry that is likely more non-LTE due to less frequent collisions. Some of those systematic deviations may be due to uncertainties in the Einstein coefficients. With the newer values, the results for 868 and 822 nm N I lines would move 10–20 K closer to those derived from the 747 nm lines.

We also checked the dependence of the excita-

tion temperature on meteor entry speed from four spectra obtained in ground campaigns outside the Leonid season. The sample consisted of three Perseid spectra obtained in ground-based campaigns in 1999 and 2000, and one Geminid spectrum obtained in December 2001. The spectra were distorted by telluric absorptions of water vapor and the atmospheric O_2 B absorption band, which affected the shape of the nitrogen band at ~ 750 nm. However, precise measurements made on the few high signal-to-noise spectra acquired to date indicated that the excitation temperatures were the same as those of faster Leonid meteors of similar brightness (Fig. 10).

DISCUSSION

Oxygen and nitrogen lines are from warm plasma, not hot

The results in this paper are contrary to previous findings on several points. Borovička (1994)

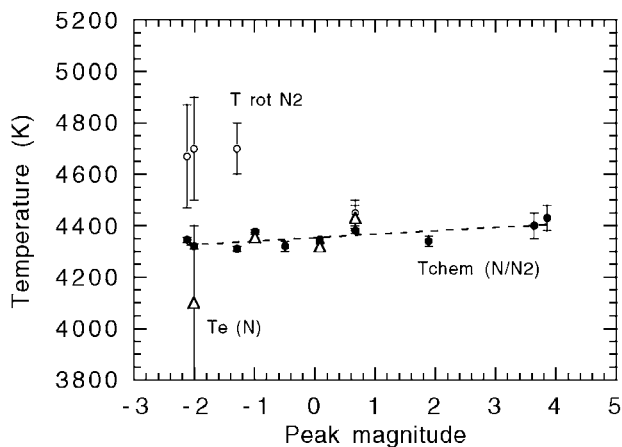


FIG. 9. Comparison of different temperature indicators, including vibrational excitation (\circ), electronic excitation (Δ), and chemical equilibrium in the air plasma (\bullet).

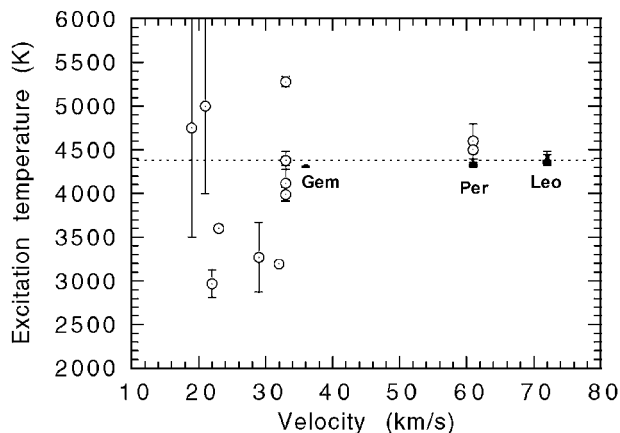


FIG. 10. Velocity dependence of meteor plasma temperature. Symbols as in Fig. 7. Speeds for natural meteoroids in elliptic orbits are in the range 11–72 km/s.

assigned the O I (777.4 nm) band “without doubt” to the high-temperature $T \sim 10,000$ K component responsible for Ca^+ and Mg^+ emissions, mainly because of atomic oxygen’s relatively high excitation energy of 10.74 eV. Indeed, Cepelcha (1971) concluded on the basis of the O I curve-of-growth analysis that the oxygen and nitrogen lines correspond to a high-temperature ($T = 14,000$ K) emission. However, Leonids and Perseids are known to display strong Ca^+ emission above about 0 magnitude. With no significant change in the O I/ N_2 and N I/ N_2 line ratio with increasing meteor brightness, this implies that the source of the hot $T \sim 10,000$ K component thought to be responsible for Ca^+ emission lacks significant air plasma emissions of atomic oxygen and nitrogen. Indeed, the match of model and observed air plasma emissions at low temperature implies that the oxygen and nitrogen lines are part of the warm $T \sim 4,400$ K component that also produces the molecular N_2 emission. Although faster meteoroids have stronger Ca^+ lines, Leonids do not show a significantly different N I/ N_2 ratio than Geminids that enter at half the speed. We conclude that the high-energy atomic lines could be observed at low temperatures in our spectra because oxygen and nitrogen atoms were so much more abundant in the air plasma than the metal atoms, not because they were excited to higher energies.

The optical thickness of the air plasma

The constant O I/ N_2 and N I/ N_2 intensity ratios also imply that the oxygen and nitrogen lines are not optically thick. It was previously thought (Cepelcha, 1964; Borovička and Majden, 1998) that the abundance of emitting atoms was sufficiently high for other atoms in the gas to absorb the emitted radiation. These earlier investigations suggested that the more intense metal atom lines of meteors as faint as +5 magnitude show such self-absorption. If self-absorbed, a progressive decrease of N I and O I line intensity relative to that of the weaker molecular N_2 band would have been expected with increasing meteor brightness. That would have produced a false increase of temperature with meteoroid mass, but the opposite (if any) was observed.

If the plasma was optically thick in the most intense lines but not in fainter lines, then the observed radiation would emerge from different depths within the plasma volume, deeper so for

the lines that originated from higher excitation energies. Within measurement uncertainty, the temperature was not a function of the energy of the upper level, as expected for an optically thick plasma (Table 3). Instead, the meteor air plasma emission was well described by an optically thin plasma for all observed lines (for meteor magnitudes of -2 and less).

We conclude that the meteor plasma does not become significantly hotter with increasing meteoroid mass over the range 10^{-5} –1 g. This conclusion is likely valid for an even wider mass range. The excitation temperatures derived from the metal atom line emissions of bright fireballs by Cepelcha (1973) give very similar temperatures (Fig. 7). These data suggest that the variation of meteor plasma emission temperature for meteoroids that range in mass from 10^{-5} to 10^6 g is at most a few 100 K.

Introducing possible different phases of meteoric air plasma

The finding that the meteoroid plasma emission temperature does not vary more than a few 100 K for meteoroids that range in mass over 11 orders of magnitude is perhaps too large a range to be consistent with our previous suggestion that a bigger or faster meteor would simply create a larger vapor cloud and thus create more plasma rather than a hotter plasma (Jenniskens *et al.*, 2000). It is unclear how the measured temperature can remain unchanged when the physical conditions change from a rarefied flow regime for 0 magnitude meteors to a continuous flow regime accompanied by the formation of a bow shock for -10 magnitude fireballs.

One possible explanation is that the plasma temperature reflects a balance between heating and cooling in the gas, a process similar to the one that causes the cool, warm, and hot phases of the interstellar medium, which have widely different temperatures but are in pressure equilibrium with each other (Begelman, 1990). Field *et al.* (1969) produced the first model for a two-phase equilibrium of the interstellar medium, in which radiative cooling is balanced by cosmic ray heating. The two phases in the model included cold dense clouds at $T \sim 100$ K and a second intercloud medium with $T \sim 10,000$ K, with a third unstable phase $T \sim 5,000$ K only expected in transient phenomena.

The characteristic temperatures of the warm and cold thermal phases are insensitive to the de-

tails of the heating processes. Instead, they reflect the rate of cooling at various temperatures $L(T)$, called the cooling curve, a function of the energies of the resonance and fine-structure lines that are responsible for the cooling of the gas. If the gas is in pressure equilibrium, the instability criterion is $(\delta L/\delta T)_p < 0$. In a meteor plasma, the heating is caused by collisional excitation of molecules with the ambient air. During radiation, there is still a significant translational velocity difference (>5 km/s) between air plasma and ambient air in the direction along the meteor's path.

A necessary and sufficient condition for the existence of a multiphase equilibrium is that the system be in pressure equilibrium and thermally unstable over a finite range of temperature. Cooling of the plasma occurs primarily through energy transfer in collisions of atoms with molecules and in radiation from those molecules. Hence, the presence of the molecules has a strong cooling effect that will tend to lower the temperature and create more molecules, thereby creating a thermally unstable condition. Thus, once there is pressure equilibrium with the surrounding medium, it is possible that different phases will form in the meteor plasma at temperatures just above the dissociation temperature of O_2 , and N_2 . While those phases may not be thermally stable, they occur because the cooling time scales are long in comparison with the occurrence of the meteor phenomenon.

If a mole fraction of 10^{-2} N_2 molecules is sufficient to create a warm phase at $T \sim 4,300$ – $4,450$ K, then a cold phase may exist at the O/O_2 equilibrium around $2,240$ – $2,300$ K. Similarly, a hot phase may be associated with the N^+/N and O^+/O ionization equilibrium at around $8,000$ K, with the atoms being more effective radiators.

The very small temperature increase with decreasing altitude (Fig. 6) is not a strong argument against such a multiphase model of the air plasma. Expansion of the plasma at higher altitudes would be expected to cause adiabatic cooling, thus affecting the equilibrium temperature.

IMPLICATIONS

The consistency of excitation temperatures makes it possible to extrapolate the observed trends to fainter meteors of sizes relevant for the mass influx at the time of the origin of life. If we allow for the weak positive trend with increasing

mass, the temperature would be $T = 4,500$ K for a typical $150 \mu\text{m}$ Leonid meteoroid (at $+12$ magnitude). Sporadic meteors with $V = 25$ km/s of similar size would have a magnitude of about $+16$ (Jenniskens *et al.*, 1998). Hence, temperatures measured for visual meteors are representative for conditions in the meteors associated with $\sim 150 \mu\text{m}$ grains responsible for the peak of the mass influx.

This $4,500$ K temperature is favorable for atmospheric chemistry and will be a factor in the chemistry of ablated organic molecules. In particular, under LTE conditions atmospheric CO_2 will dissociate into CO and O , and subsequently, CO will dissociate into its atoms. Between temperatures of about $3,600$ and $5,000$ K, the carbon atoms will react with N_2 and other molecules to form relatively high abundances of C_2 , C_3 , and CN (Jenniskens *et al.*, 2000). Yields are highest for $T \sim 4,100$ K. The atmospheric carbon atoms can also react with meteoric organic matter to form longer carbon chains. At the same time, nitrogen radicals peak in abundance above $4,000$ K and can react with other meteoric organic molecules to form stable $-CN$ and $C=O$ bonds in reactions with oxygen atoms and CO_2 molecules. Thus, organic compounds can be created that are enriched in nitrogen and oxygen compared with the organic matter typically found in the (micro-) meteorites that are studied in many laboratory investigations. How much this process counteracts the extraction of carbon by reaction with O and OH radicals needs to be investigated in chemical modeling. Such work is outside the scope of this paper.

The picture could significantly change if our hypothesis of a multiphase medium is correct. In that case, the meteor plasma temperature may be different in a different atmosphere. If the plasma temperature is lower, this would favor the survival of organic molecules that are ablated from the meteoroid. On the other hand, the NO fixation rate, which is mostly determined by oxygen atom attack with nitrogen molecules, would be significantly lower, perhaps to the point of being negligible.

In a Mars-like CO_2 -rich atmosphere on the early Earth, an equilibrium around $2,170$ – $2,230$ K might have been established just above the CO/CO_2 dissociation threshold or above the CO/C threshold. The latter is more likely, however, because both CO and CO_2 are good thermal emitters, in which case the temperature would

have been similar to that observed in today's Earth atmosphere.

We conclude that the excitation and chemical equilibrium temperatures in meteor plasma remain in a narrow range for a wide range of entry speed and initial mass. Whether the reason for this is the presence of a multiphase equilibrium can be tested, for example, in future meteor observations on Mars or in laboratory experiments of artificial meteors in CO₂- and O₂-rich atmospheres.

ACKNOWLEDGMENTS

The ASTRO instrument was developed with support of NASA Ames Research Center's Director's Discretionary Fund in preparation of the Leonid MAC missions. We thank Mike Koop and Gary Palmer for technical support. The 2001 Leonid MAC was sponsored by NASA's Astrobiology ASTID (Astrobiology Instrument and Development) and Planetary Astronomy programs. The mission was executed by the USAF 418th Flight Test Squadron. This work meets with objective 3.1 of NASA's Astrobiology Roadmap (Des Marais *et al.*, 2003).

ABBREVIATIONS

CCD, charge coupled device; LTE, local thermodynamic equilibrium; MAC, Multi-Instrument Aircraft Campaign; UT, universal time.

REFERENCES

- Anders, E. (1989) Pre-biotic organic matter from comets and asteroids. *Nature* 342, 255–257.
- Begelman, M.C. (1990) Thermal phases of the interstellar medium in galaxies. In *The Interstellar Medium in Galaxies*, edited by H.A. Thronson, Jr. and J.M. Shull, Kluwer Academic Publishers, Dordrecht, The Netherlands, pp. 287–304.
- Borovička, J. (1993) A fireball spectrum analysis. *Astron. Astrophys.* 279, 627–645.
- Borovička, J. (1994) Two components in meteor spectra. *Planet. Space Sci.* 42, 145–150.
- Borovička, J. and Betlem, H. (1997) Spectral analysis of two Perseid meteors. *Planet. Space Sci.* 45, 563–575.
- Borovička, J. and Majden, E.P. (1998) A Perseid meteor spectrum. *J. R. Astron. Soc. Canada* 92, 153–156.
- Borovička, J. and Spurný, P. (1996) Radiation study of two very bright terrestrial bolides and an application to the comet S-L 9 collision with Jupiter. *Icarus* 121, 484–510.
- Borovička, J. and Weber, M. (1996) An alpha-Capricornid meteor spectrum. *WGN J. Int. Meteor. Org.* 24, 30–32.
- Borovička, J., Popova, O.P., Golub, A.P., Kosarev, I.B., and Nemtchinov, I.V. (1998) Bolides produced by impacts of large meteoroids into the Earth's atmosphere: Comparison of theory with observations. II. Beneov bolide spectra. *Astron. Astrophys.* 337, 591–602.
- Boyd, I.D. (2000) Computation of atmospheric entry flow about a Leonid meteoroid. *Earth Moon Planets* 82–83, 93–108.
- Ceplecha, Z. (1964) Study of a bright meteor flare by means of emission curve of growth. *Bull. Astron. Inst. Czech.* 15, 102–112.
- Ceplecha, Z. (1965) Complete data on bright meteor 32281. *Bull. Astron. Inst. Czech.* 16, 88–100.
- Ceplecha, Z. (1967) Spectroscopic analysis of iron meteoroid radiation. *Bull. Astron. Inst. Czech.* 18, 303–310.
- Ceplecha, Z. (1968) Meteor spectra (survey paper). In *International Astronomical Union Symposium No. 33: Physics and Dynamics of Meteors*, edited by L. Kresák and P.M. Millman, D. Reidel Publishing Co., Dordrecht, The Netherlands, pp. 73–83.
- Ceplecha, Z. (1971) Spectral data on terminal flare and wake of double-station meteor No. 38421 (Ondrejov, April 21, 1963). *Bull. Astron. Inst. Czech.* 22, 219–304.
- Ceplecha, Z. (1973) A model of spectral radiation of bright fireballs. *Bull. Astron. Inst. Czech.* 24, 232–242.
- Chyba, C.F. and Sagan, C. (1992) Endogenous production, exogenous delivery and impact shock synthesis of organic molecules: An inventory for the origins of life. *Nature* 355, 125–132.
- Cook A.F. and Millman P.M. (1954) Photometric analysis of a spectrogram of a Perseid meteor. *Contrib. Dominion Observatory* 2, 250–270.
- Des Marais, D.J., Allamandola, L.J., Benner, S.A., Deamer, D., Falkowski, P.G., Farmer, J.D., Hedges, S.B., Jakosky, B.M., Knoll, A.H., Liskowsky, D.R., Meadows, V.S., Meyer, M.A., Pilcher, C.B., Nealson, K.H., Spormann, A.M., Trent, J.D., Turner, W.W., Woolf, N.J., and Yorke, H.W. (2003) The NASA Astrobiology Roadmap. *Astrobiology* 3, 219–235.
- Field, G.B., Goldsmith, D.W., and Habing, H.J. (1969) Cosmic-ray heating of the interstellar gas. *Ap. J. Lett.* 155, L149–L154.
- Harvey, G.A. (1971) The calcium H- and K-line anomaly in meteor spectra. *Astrophys. J.* 165, 669–671.
- Harvey, G.A. (1973) Spectral analysis of four meteors. In *National Aeronautics and Space Administration SP 319: Evolutionary and Physical Properties of Meteoroids, Proceedings of IAU Colloquium 13*, edited by C.L. Hemenway, P.M. Millman, and A.F. Cook, NASA, Washington, DC, pp. 103–129.
- Herzberg, G. (1950) *Spectra of Diatomic Molecules*, D. Van Nostrand Co., New York.
- Jenniskens, P. and Butow, S.J. (1999) The 1998 Leonid multi-instrument aircraft campaign—an early review. *Meteoritics Planet. Sci.* 34, 933–943.
- Jenniskens, P. and Russell, R.W. (2003) The 2001 Leonid

- Multi-Instrument Aircraft Campaign—an early review. *ISAS Rep. SP 15*, 3–15.
- Jenniskens, P. and Stenbaek-Nielsen, H.C. (2004) Meteor wake in high frame-rate images—implications for the chemistry of ablated organic compounds. *Astrobiology* **4**, 95–108.
- Jenniskens, P., de Lignie, M., Betlem, H., Borovička, J., Laux, C.O., Packan, D., and Krüger, C.H. (1998) Preparing for the 1998/99 Leonid storms. *Earth Moon Planets* **80**, 311–341.
- Jenniskens, P., Wilson, M.A., Packan, D., Laux, C.O., Boyd, I.D., Popova, O.P., and Fonda, M. (2000) Meteors: A delivery mechanism of organic matter to the early Earth. *Earth Moon Planets* **82-83**, 57–70.
- Jenniskens, P., Schaller, E.L., Laux, C.O., Schmidt, G., and Rairden, R.L. (2004) Meteors do not break exogenous organic molecules into high yields of diatomics. *Astrobiology* **4**, 67–79.
- Laux, C.O. (1993) Optical diagnostics and radiative emission of air plasmas [Ph.D. Dissertation], HTGL Report T288, Stanford University, August 1993, Stanford University, CA.
- Love, S.G. and Brownlee, D.E. (1993) A direct measurement of the terrestrial mass accretion rate of cosmic dust. *Science* **262**, 550–553.
- Park, C. S., Newfield, M.E., Fletcher, D.G., Gökçen, T., and Sharma, S.P. (1997). Spectroscopic emission measurements within the blunt-body shock layer in an arc-jet flow. In *AIAA 97-0990*, American Institute of Aeronautics and Astronautics, Reston, VA, p. 18.
- Popova, O.P., Sidneva, S.N., Shuvalov, V.V., and Strelkov, A.S. (2000) Screening of meteoroids by ablation vapor in high-velocity meteors. *Earth Moon Planets* **82-83**, 109–128.

Address reprint requests to:

Dr. Peter Jenniskens

Center for the Study of Life in the Universe

SETI Institute

2035 Landings Drive

Mountain View, CA 94043

E-mail: pjenniskens@mail.arc.nasa.gov